

3 Voltage-Gated Ion Channels

Francisco Bezanilla

3.1 Introduction

The bit of information in nerves is the action potential, a fast electrical transient in the transmembrane voltage that propagates along the nerve fiber. In the resting state, the membrane potential of the nerve fiber is about -60 mV (negative inside with respect to the extracellular solution). When the action potential is initiated, the membrane potential becomes less negative and even reverses sign (overshoot) within a millisecond and then goes back to the resting value in about 2 ms, frequently after becoming even more negative than the resting potential. In a landmark series of papers, Hodgkin and Huxley studied the ionic events underlying the action potential and were able to describe the conductances and currents quantitatively with their classical equations (Hodgkin and Huxley, 1952). The generation of the rising phase of the action potential was explained by a conductance to Na^+ ions that increases as the membrane potential is made more positive. This is because, as the driving force for the permeating ions (Na^+) was in the inward direction, more Na^+ ions come into the nerve and make the membrane more positive initiating a positive feedback that depolarizes the membrane even more. This positive feedback gets interrupted by the delayed opening of another voltage-dependent conductance that is K-selective. The driving force for K^+ ions is in the opposite direction of Na^+ ions, thus K^+ outward flow repolarizes the membrane to its initial value. The identification and characterization of the voltage-dependent Na^+ and K^+ conductances was one of the major contributions of Hodgkin and Huxley. In their final paper of the series, they even proposed that the conductance was the result of increased permeability in discrete areas under the control of charges or dipoles that respond to the membrane electric field. This was an insightful prediction of ion channels and gating currents.

Many years of electrical characterization, effects of toxins on the conductances, molecular biological techniques, and improvement of recording techniques led to the identification of separate conducting entities for Na^+ and K^+ conductances. These conductances were finally traced to single-membrane proteins, called ion channels, that can gate open and closed an ion conducting pathway in response to changes in membrane potential.

Francisco Bezanilla

3.2 Voltage-Dependent Ion Channels Are Membrane Proteins

The first voltage-dependent ion channel that was isolated and purified was extracted from the eel electroplax where there is a large concentration of Na^+ channels (Agnew et al., 1978). Several years later, the sequence of the eel Na^+ channel was deduced from its mRNA (Noda et al., 1984). The first K^+ channel sequence was deduced from the *Shaker* mutant of *Drosophila melanogaster* (Tempel et al., 1987). These initial sequences were the basis to subsequent cloning of a large number of Na^+ , K^+ , and Ca^{2+} channels in many different species. Hydropathy plots were helpful in deciding which parts of the sequence were transmembrane or intra- or extracellular. A basic pattern emerged from all these sequences: the functional channels are made up of four subunits (K^+ channels) or one protein with four homologous domains (Na^+ and Ca^{2+} channels). Each one of the domains or subunits has six transmembrane segments and a pore loop (see Fig. 3.1). The fifth and sixth transmembrane segments (S5 and S6) and the pore loop were found to be responsible for ion conduction. The

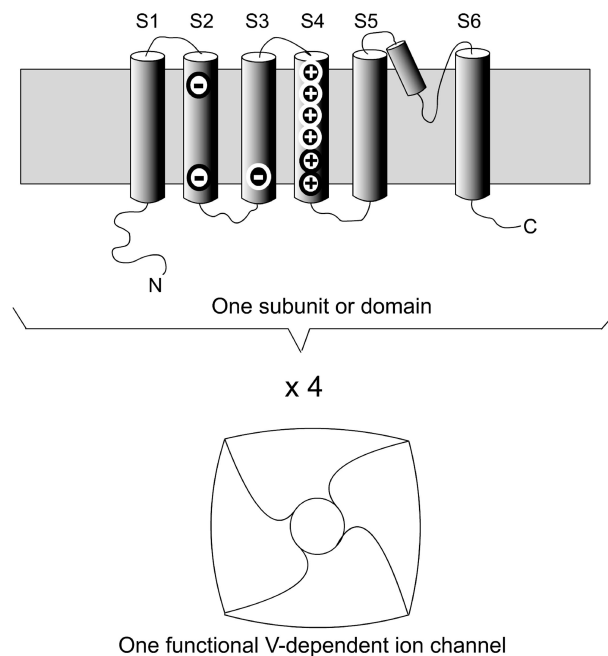


Fig. 3.1 The general architecture of voltage-gated channels. Top part shows the basic subunit (or domain in the case of Na^+ and Ca^{2+} channels). The gray background represents the lipid bilayers. The cylinders are transmembrane segments. The region between S5 and S6 forms the pore. Segments 1 through 4 are called the voltage sensor part of the channel. The + or - signs in white indicate charges that have been implicated in voltage sensing. In the bottom, a schematic view of the channel from the outside showing the assembled four subunits or domains.

3. Voltage-Gated Ion Channels

fourth transmembrane segment (S4) contains several basic residues, arginines or lysines and was initially postulated to be the voltage sensor (Noda et al., 1984). In addition, S2 and S3 contain acidic residues such as aspartate and glutamate. Most of the channels have additional subunits that modify the basic function but they are not necessary for voltage sensing and ion conduction.

3.3 The Parts of the Voltage-Dependent Channel

We think of voltage-dependent channels as made of three basic parts: the *voltage sensor*, the *pore* or *conducting pathway*, and the *gate*. These three parts can be roughly mapped in the putative secondary structure (Fig. 3.1). The pore and the gate are in the S5-loop-S6 region and the voltage sensor in the S1–S4 region. As the conduction is dependent on the voltage across the membrane, a useful analogy is a field effect transistor (FET; see Fig. 3.1). If we take a typical voltage-dependent K channel, its voltage sensor corresponds to the gate of a p-channel FET, the conducting pathway of the ion channel corresponds to the p-channel (Fig. 3.2) and the gate of the channel is the space charge in the p-channel. As we will see below, this analogy is useful to discuss the parts of the channel but it cannot be pushed very far because, although the functions are similar, the actual mechanisms are quite different.

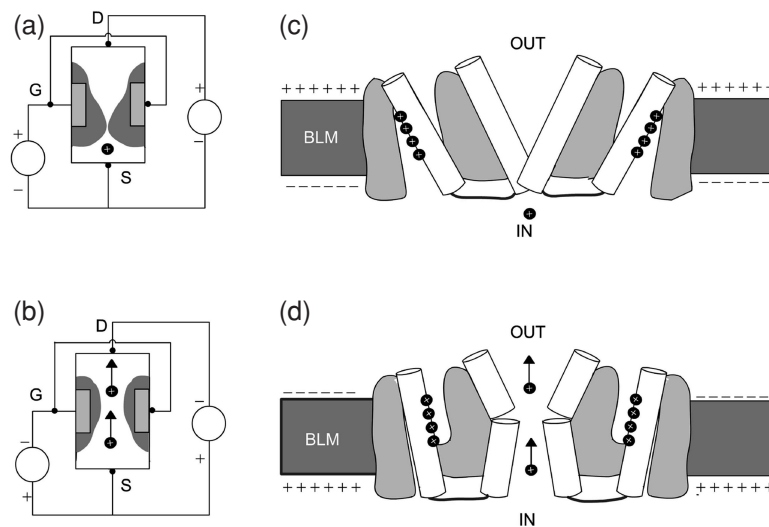


Fig. 3.2 A comparison between a field effect transistor and a voltage-gated ion channel. The FET transistor is represented as a p-channel device to make a closer analogy to a cation selective voltage-gated channel. (a) and (c) are the closed states; (b) and (d) are the open states. Notice that, in contrast with the FET, the gate in the voltage-gated channel indicates the actual point of flow interruption. In the FET, D is the drain, S is the source, G is the gate. For details see text.

Francisco Bezanilla

3.3.1 The Conducting Pathway

Living cells, and in particular nerve fibers, are surrounded by a thin membrane made of a bimolecular layer of lipids. The permeability of ions through the lipid bilayer is extremely low because it takes a large amount of energy to put a charged ion species inside the low-dielectric constant lipid bilayer (Parsegian, 1969). The conducting pathway of ion channels lowers that energy barrier by providing a favorable local environment and thus allowing large flows under an appropriate driving force. Details of the ion conduction pore structure, conductance, and selectivity are covered in other chapters in this ~~handbook (XXX)~~. What is important to emphasize here is that the ion flow is proportional to the driving force for the selected ion. The driving force corresponds to the difference between the voltage applied, V and the voltage at which there is no flow, or reversal potential E . If the channel is perfectly selective to one type of ion, say K^+ , then E is the Nernst potential, otherwise E is predicted by the Goldman–Hodgkin and Katz equation that considers concentrations and relative permeabilities. Knowing the conductance of the conducting pathway γ , we can compute the current flow i through the open conducting pore as,

$$i = \gamma(V - E). \quad (3.1)$$

The i - V curve of an open channel may be nonlinear because in general, γ is voltage dependent.

3.3.2 The Gate

The ion conduction through the pore may be interrupted by closing a gate (see Fig. 3.2). Thermal fluctuations will close and open the gate randomly and the current will have interruptions. In voltage-dependent channels, the probability that the gate is open, P_o , depends on the membrane potential. In the majority of voltage-dependent Na^+ , K^+ , and Ca^{2+} channels from nerve and muscle the P_o increases with membrane depolarization (i.e., decrease in the resting potential). There are a few cases, such as Kat1 channel, where P_o increases on hyperpolarization.

The operation of the gate can be seen by recording the current flowing through a single ion channel. This is possible with the patch clamp technique (Hamill et al., 1981) that records currents from a very small patch of membrane with a small glass pipette and a low-noise system that can resolve currents in the order 1 pA. An example of the operation of one K^+ channel is shown in a simulation in Fig. 3.3. As the internal concentration of K^+ is more than 10 times higher in the cell as compared to the extracellular space, the reversal potential E for K^+ channels is around -80 mV. Starting with a negative membrane potential (-100 mV), the channel is closed most of the time. A depolarizing voltage pulse to -30 mV increases the open probability and the channel spends some time in the open state (Fig 3.3a). As we are dealing with one molecule, thermal fluctuations will generate different responses for each repetition of the same pulse (four of such are shown in the figure). A larger depolarization

Au: Please check and provide the relevant information here.



3. Voltage-Gated Ion Channels

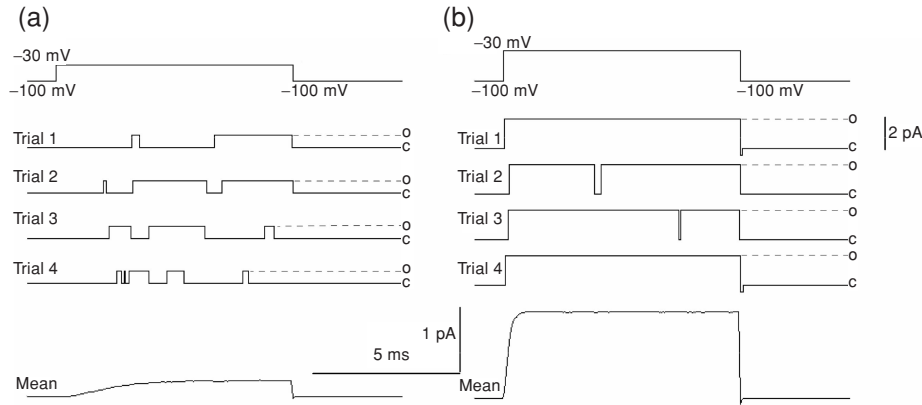


Fig. 3.3 Time course of single channel and macroscopic ionic currents. The applied voltage is in the top trace and the current recorded through one channel is shown for four different trials. The mean current is the result of thousands of trials. (a) Small depolarization to -30 mV, open the channel infrequently. (b) A large depolarization (to $+30$ mV) opens the channel most of the time. c is the closed state and o is the open state.

($+30$ mV) increases the P_o even more by increasing the open times and decreasing the closed times, as seen in Fig. 3.3b. Notice also that the time elapsed between the start of the pulse and the first opening (first latency) is decreased for the larger depolarization. Apart from increasing the open times, the magnitude of the current through the pore was increased by the larger depolarization. This is because the V applied is now further away from E , increasing the driving force for ion movement. Thus, this increase in current is not a result of increasing P_o but is just a passive property of the open pore. An average of several thousands of repetitions gives us the macroscopic ionic currents. Provided the channels do not interact, the average of thousands of repetitions is the same as having thousands of channels operating simultaneously. The bottom trace (labeled mean) in Fig. 3.3a and 3.3b shows the macroscopic currents for -30 and $+30$ mV, respectively. Notice that the turn-on kinetics is faster for a more positive potential and that the current magnitude is also increased. The kinetics change is the result of an increased P_o while the magnitude increase is the result of both increased P_o and driving force. We can now write the expression for the macroscopic current as,

$$I = P_o(V, t)N\gamma(V - E), \quad (3.2)$$

where N is the channel density and $P_o(V, t)$ is the voltage and time-dependent open probability.

3.3.3 The Voltage Sensor

How does P_o become voltage dependent? It is clear that to detect changes in membrane potential a voltage sensor is needed. The electric field in the bilayer could

Francisco Bezanilla

be detected by electric or magnetic charges or dipoles that change their position according to changes in the field. As there is no evidence of magnetic charges, electric charges or dipoles remain as the prime candidates. We will see below that the actual charges involved in voltage sensing have been identified and a schematic representation of their relocation is shown in Fig. 3.2b. In the resting (hyperpolarized) condition, the membrane is negative inside and the positive charges are located in contact with the interior of the cell. Upon depolarization, the positive charges are driven toward the outside. This movement in the electric field has two consequences: it is coupled to the gate resulting in pore opening (Fig. 3.2b) and the charge translocation produces another membrane current that is transient in nature, called *gating current*. It is called gating current because it ultimately gates the channel open and close and it is transient because the charge locations are bound to limiting positions as they are tethered to the protein.

3.4 Gating Charge and the Voltage Sensor

An understanding of the voltage sensor requires a characterization of the gating charge movement and a correlation of that movement to structural changes in the protein. In this section, we will address two functional questions. The first question is what are the kinetics and steady state properties of the gating charge movement and how does this charge movement relate to channel activation. The second is how many elementary charges move in one channel to fully activate the conductance and how does this movement occur in one channel.

3.4.1 The Gating Currents and the Channel Open Probability

The movement of charge or dipole reorientation is the basic mechanism of the voltage sensor and was predicted by Hodgkin and Huxley (1952). Gating currents are transient and they only occur in the potential range where the sensor responds to the electric field, therefore they behave like a nonlinear capacitance. In addition, as gating currents are small, to record them it is necessary to decrease or eliminate the ionic currents through the pore and eliminate the normal capacitive current required to charge or discharge the membrane. This is normally accomplished by applying a pulse in the voltage range that activates the current and then subtract another pulse or pulses in the voltage range that does not activate the currents to eliminate the linear components (Armstrong and Bezanilla, 1973; Keynes and Rojas, 1974). Using these subtraction techniques, the kinetics of Na^+ gating currents were studied in detail in squid giant axon and other preparations where a high-channel density was found. The combination of gating currents, macroscopic ionic currents, and single-channel recordings were used to propose detailed kinetic models of channel operation (see Vandenberg and Bezanilla, 1991). When voltage-dependent channels were cloned and expressed in oocytes or cell lines, it was possible to achieve large channel densities on the surface membrane and study those channels in virtual absence of

3. Voltage-Gated Ion Channels

currents from other channels. In comparison to the currents in natural tissues such as the squid giant axon, the expression systems gating currents were much larger and made the recording easier and cleaner. In addition, the study of the pore region gave us the possibility of mutating the channel protein to eliminate ionic conduction but maintaining the operation of the gating currents (Perozo et al., 1993). We can illustrate the basic features of gating currents and their relation to ionic currents in recordings from Shaker K^+ channels with fast inactivation removed (Shaker-IR) as shown in Fig. 3.4a.

In this figure, two separate experiments are shown. The top traces are the time course of the ionic currents recorded during pulses that range from -120 to 0 mV, starting and returning to -90 mV. The bottom traces are gating currents recorded for the same set of pulses from Shaker-IR with a mutation that changes a tryptophan into a phenylalanine in position 434 (W434F) that renders the pore nonconducting (Perozo et al., 1993). Several features that are characteristic of most voltage-dependent channels can be observed. First, the ionic currents do not show significant activation for potential more negative than -40 mV while the gating currents are visible for all the pulses applied, implying that there is charge displacement in a region of potentials where most of the channels are closed. Second, the time course of activation of the ionic current is similar to the time course of decay of the gating current. Third, the time course of the return of the charge (gating current “tail”) changes its kinetics drastically when returning from a pulse more positive than -40 mV, which is precisely the potential at which ionic currents become clearly visible. The gating tails are superimposable for potentials more positive than -20 mV, showing that most of the charge has moved at -20 mV. The total charge moved at each potential may be computed as the time integral of the gating current for each pulse. As we will see below, it is possible to estimate the total charge moved per channel molecule, therefore the voltage dependence of the charge moved can be plotted as shown in Fig. 3.4b. Knowing the number of channels present (see below), using Eq. 3.2, it is possible to estimate the voltage dependence of P_o , as shown in the same figure. Fig. 3.4b establishes the relationship between the charge movement and channel opening and clearly shows that the opening of the channel is not superimposable with charge movement as expected from a simple two state model. A striking feature of these plots is that the $Q(V)$ relation is displaced to the left of the $P_o(V)$ curve so that there is quite a large charge movement in a region where the P_o is essentially zero. This is an expected feature of a channel that requires several processes to occur to go from closed to open, such as the classical Hodgkin and Huxley model where four independent particles are needed to be simultaneously in the active position for the channel to be open.

Current recordings of the type shown in Fig. 3.4a can be used to formulate kinetic models of channel gating. These models are normally written as a collection of closed and open states interconnected with rate constants that, in general, are a function of the membrane potential. Initially, kinetic models were developed from the macroscopic ionic currents only (Hodgkin and Huxley, 1952). The addition of single-channel recordings and gating current recordings imposes several constraints

Francisco Bezanilla

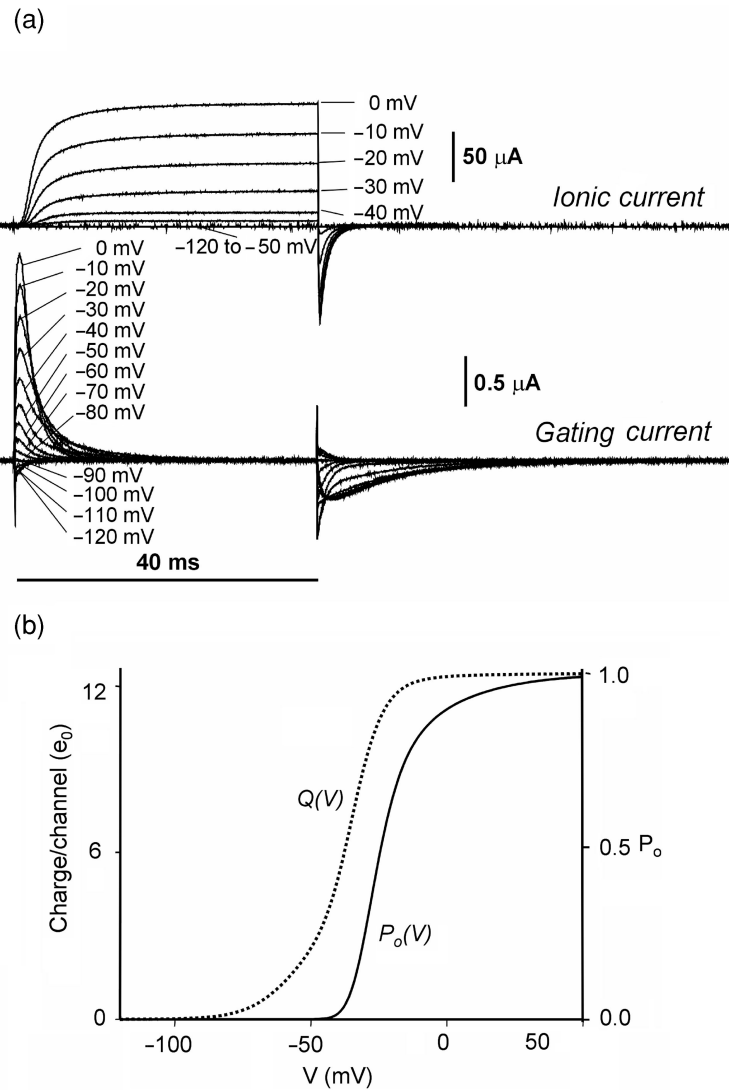


Fig. 3.4 Ionic and gating currents in Shaker-IR K^+ channel. (a) Top traces, time course of ionic currents for pulses to the indicated potentials starting and returning to -90 mV. Bottom traces, time course of the gating currents for the pulses indicated. Notice the difference in the amplitude calibration for ionic as compared to gating currents. (b) The voltage dependence of the open probability, P_o , and the charge moved per channel, $Q(V)$. For details see text.

in the possible models and in the parameters fitted, thus obtaining a more robust representation of the kinetic parameters that characterize the channel.

The common assumption in kinetic models is that the movement of the charge or dipole in the field has a finite number of low-energy positions and energy barriers

3. Voltage-Gated Ion Channels

in between them. According to kinetic theory, the transition rates across the energy barrier are exponentially related to the negative of the free energy amplitude of the barrier. This free energy contains nonelectrical terms and an electrical term such that the membrane voltage can either increase or decrease the total energy barrier resulting in changes in the forward and backward rates of crossing the barriers. There are multiple examples in the literature with varied levels of complexity that describe well the kinetic and steady state properties of several types of voltage-dependent channels (see for example, Vandenberg and Bezanilla, 1991; Bezanilla et al., 1994; Zagotta et al., 1994; Schoppa and Sigworth, 1998).

A more general approach to modeling is based on a representation of a landscape of energy using the charge moved as the reaction coordinate. In this type of modeling, the above-mentioned discrete kinetic models are also represented when the landscape of energy has surges that exceed $4kT$ (Sigg et al., 1999).

When gating currents are recorded with high-bandwidth new components are observed (Sigg et al., 2003). Figure 3.5a shows a typical gating current trace recorded with a bandwidth of 10 kHz. Notice that before the initial plateau and decay of the

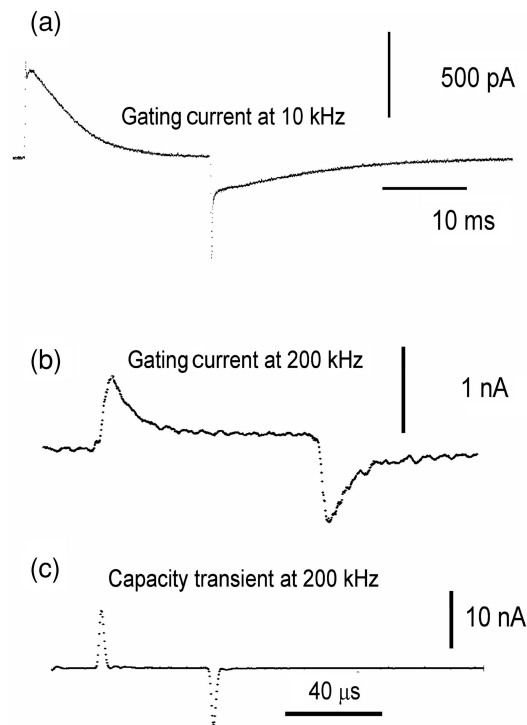


Fig. 3.5 The early component of the gating current. (a) Gating current recorded at 10 kHz bandwidth. (b) Gating current recorded at 200 kHz bandwidth. Notice the differences in the amplitude and time scales. (c) The time course of the charging of the membrane capacitance for the experiment in part (b). Recordings done in collaboration with Dr. Enrico Stefani.

Francisco Bezanilla

gating current there is a brief surge of current. When the bandwidth is increased to 200 kHz, the first surge of current is the predominant amplitude as shown in the fast time scale recording of Fig. 3.5b. The large spike of current is followed by a long plateau of current that corresponds to the plateau observed at 10 kHz in Fig. 3.5a. However, the area spanned by the large spike is a very small fraction of the total charge moved during the entire time course of the gating current. The interpretation of this early component is best understood using the representation of the gating charge moving in a landscape of energy that undergoes a change in tilt when the membrane potential is changed such that the charge advances in its initial energy well before making the jump across the first energy barrier. Using this approach, Sigg et al. (2003) computed the viscosity encountered by the gating charge in its well of energy.

3.4.1.1 What Have We Learned with Kinetic Modeling?

In fact a great deal. It is now clear that voltage-dependent channels have multiple closed states and, in some cases several open states. In general, the opening of the gate requires all four subunits to be activated, although there are cases where intermediate states have been observed (see Chapman and VanDongen, 2005). Each subunit undergoes several transitions before reaching the active state and in the case of K^+ channels they do not seem to interact until the final step that opens the channel (Horn et al., 2000; Mannuzzu and Isacoff, 2000). The situation is different in the case of the muscle Na^+ channel where site-directed fluorescence studies show that interdomain interactions are manifested prior to channel opening (Chanda et al., 2004). Kinetic modeling has given us a picture of the channel in terms of channel physical states with transitions between them that are regulated by voltage. Kinetic modeling is a critical step in developing a physical model of channel operation because all the predicted features of channel function should be reproduced by the structure of the protein and its voltage-induced conformational changes.

3.4.2 Gating Charge per Channel

When the gating charge moves within the electric field we detect a current in the external circuit. The time integral of that current represents the charge moved times the fraction of the field it traverses, therefore our measurement of gating charge does not represent the exact number of charges displaced because it includes the arrangement of the electric field. We must keep this in mind, when we represent the reaction coordinate of the activation of the channel in the variable q . A channel evolves from $q = 0$ to $q = z_T$ traversing many closed and/or open states. Activation of the channel corresponds to the opening of the pore and, analogous to the chemical potential, we define the *activation potential* as

$$W_a = -kT \ln P_o. \quad (3.3)$$

3. Voltage-Gated Ion Channels

Then, the activation charge displacement q_a corresponds to the negative gradient of the activation potential,

$$q_a = -\frac{dW_a}{dV} = kT \frac{d \ln P_o}{dV}. \quad (3.4)$$

The equilibrium probabilities in each physical state of the channel can be explicitly written using the Boltzmann distribution knowing the potential of mean force F_i for each state i . Then, by assigning open or closed (or intermediate states) conductances to every state, we can write an expression for P_o that includes the voltage dependence of F_i . The final result of the derivation (Sigg and Bezanilla, 1997) gives a relation between $q(V)$, q_a , z_T and the charge moving between open states q_l ,

$$q(V) = z_T - q_a - q_l. \quad (3.5)$$

Note that $q(V)$ is the $Q-V$ curve shown in Fig. 3.5. This result is general and includes cases with any number of open and closed states connected in any arbitrary manner. If there is no charge movement between open states ($q_l = 0$), then the $Q-V$ curve superimposes on q_a . In addition, it is possible to estimate z_T , the total charge per channel, by taking the limiting value of q_a that makes $q(V)$ go to zero. In the typical case of a channel that closes at negative potentials, we obtain

$$z_T = \lim_{V \rightarrow -\infty} kT \frac{d \ln P_o}{dV}, \quad (3.6)$$

a result that was first obtained by (Almers, 1978) for the special case of a sequential series of closed states ending in an open state. This method has been applied to several types of voltage-dependent channels and the charge per channel obtained ranges between 9 and 14 e_0 (Hirschberg et al., 1996; Noceti et al., 1996; Seoh et al., 1996).

Another way to estimate the charge per channel is to measure the maximum charge from the $Q-V$ curve and divide by the number of channels present, Q/N method. The number of channels can be estimated by noise analysis (Schoppa et al., 1992) or by toxin binding (Aggarwal and MacKinnon, 1996). The value of charge per channel estimated by the Q/N method was 12 to 13 e_0 for the Shaker K^+ channel, a value that was not different from the value obtained by the limiting slope method (Seoh et al., 1996). As the limiting slope measures only the charge involved in opening the channel, the agreement between the two methods imply that in case of the Shaker channel there is no peripheral charge. The large value of 12 to 13 e_0 per channel explains the very steep voltage dependence of the superfamily of voltage-gated ion channels. At very negative V , q_a has a linear dependence on V , so that P_o is exponential in V , such that it increases by e in only 2 mV:

$$P_o \propto \exp(z_T V / kT). \quad (3.7)$$

Francisco Bezanilla

This very steep voltage dependence explains why the P_o-V curve of Fig. 3.4b shows no visible P_o at potentials more negative than -40 mV: in fact there is a finite value of P_o of less than 10^{-5} at potentials as negative as -100 mV.

Voltage-dependent channels that have several open states with charge moving between them ($q_l \neq 0$), show plots of P_o-V that may not be used to compute z_T . One example is the maxi K^+ channel, activated by voltage and Ca^{++} , that shows a P_o-V curve with a slope that decreases as the potential is made more negative. This result is consistent with the multiple-state allosteric model proposed for this channel (Horrigan et al., 1999).

3.4.2.1 Gating Current of One Channel

The previous paragraph shows that we can estimate the total charge that moves in one channel but does not give any ideas of how that charge movement occurs at the single-channel level. Two limiting cases can be proposed. In one case, the time course of the gating current is just a scaled down version of the macroscopic gating current shown in Fig. 3.4. The other case assumes that the charge movement occurs in large elementary jumps and that the macroscopic gating current is the sum of those charge shots. Figure 3.6 is a simulation of the gating shots expected from a channel that is made up of four identical subunits, each having two states: resting and active. The resting position is favored at negative potentials while the active position is favored at positive potentials and there is a large energy barrier that separates the resting from the active position. At negative potential, the charge will cross the energy barrier rarely, due to thermal motion. As the membrane potential is made more positive the energy landscape tilts and the barrier decreases. Then the probability of crossing the barrier increases and discrete jumps occur. The jump of the charge generates a very fast current transient (shown in the figure as vertical bars) whose duration is limited in practice by the frequency response of the recording system. The simulation shows one trial starting at -100 mV and pulsing to 0 mV. Notice that immediately after the pulse, each of the four subunits (I_{g1} through I_{g4}) responds at different times and that there are spontaneous reverse currents in I_{g1} and I_{g2} . The ionic channel current only appears when all four subunits have made the transition as shown in I_{single} . When several trials are averaged, the gating shots produce the macroscopic gating current (Average I_g) and the average of the single-channel currents produce the Average I_{ionic} . In principle, if the charge is moving in discrete packets, it should be possible to detect those elementary events as it has been possible to detect the elementary events of pore conduction. The problem is that, as those events are very fast and extremely small, they are not detectable above background noise with present techniques. However, if those events do exist, they should produce detectable fluctuations in the gating currents recorded from a relatively small number of channels. In the simulation shown in Fig. 3.6, the average I_g shows excess noise during the decay of the gating current. This noise is the result of the contribution of the elementary shots shown for only one trial in the same figure. To detect this excess noise and do the fluctuation analysis, the same voltage pulse is

3. Voltage-Gated Ion Channels

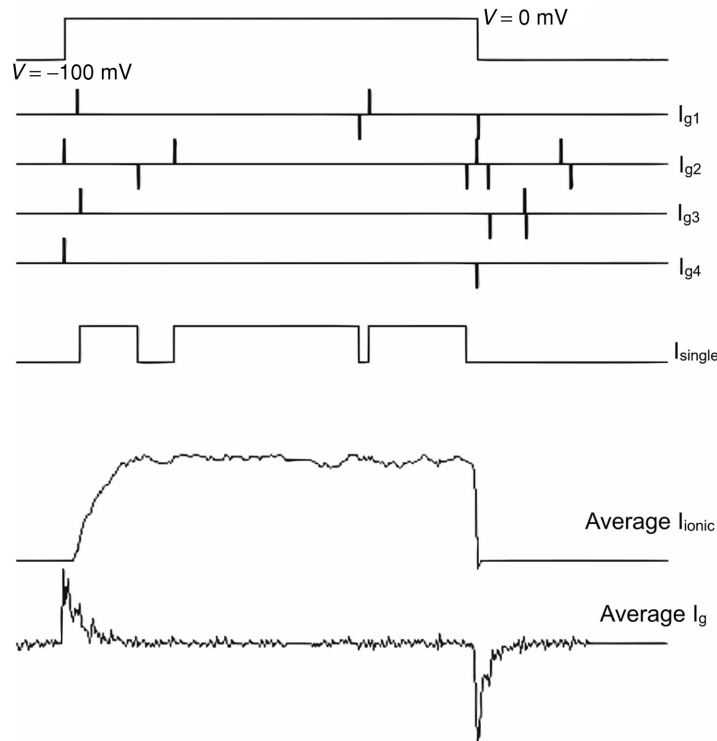


Fig. 3.6 Time course of the gating shots, single-channel current and macroscopic ionic and gating currents. The applied voltage is in the top trace. I_{g1} through I_{g4} represent the current recording of the gating shots for each one of the four subunits. I_{single} represents the time course of the ionic current for one trial as a result of the movements of the four sensors. Average I_{ionic} is the average of the single-channel currents for 80 trials. Average I_g is the average of all the subunits gating shots for a total of 80 trials.

repeated many times and a large number of gating current traces are recorded. From these traces, an ensemble mean value and an ensemble variance are obtained that allows the estimation of the elementary event (Fig. 3.7)

Gating current noise analysis was first done in Na^+ channels expressed in oocytes (Conti and Stuhmer, 1989) where indeed it was possible to detect fluctuations that were used to estimate an elementary charge of $2.2 e_0$. A similar analysis was done in Shaker-IR K^+ channel (Sigg et al., 1994) and the elementary charge was found to be $2.4 e_0$. This value corresponds to the maximum shot size and if it were per subunit it would account for only $9.6 e_0$ or $3.6 e_0$ less than the $13 e_0$ measured for the whole channel. This means that there is a fraction of the total charge that produces less noise and then it may correspond to smaller shots or even a continuous process. Figure 3.7 shows the mean and variance for a large pulse (to $+30$ mV) and a smaller depolarization (to -40 mV). For the small depolarization (Fig. 3.6b), gating current noise increases by the time that more than half of the charge has moved. This

Francisco Bezanilla

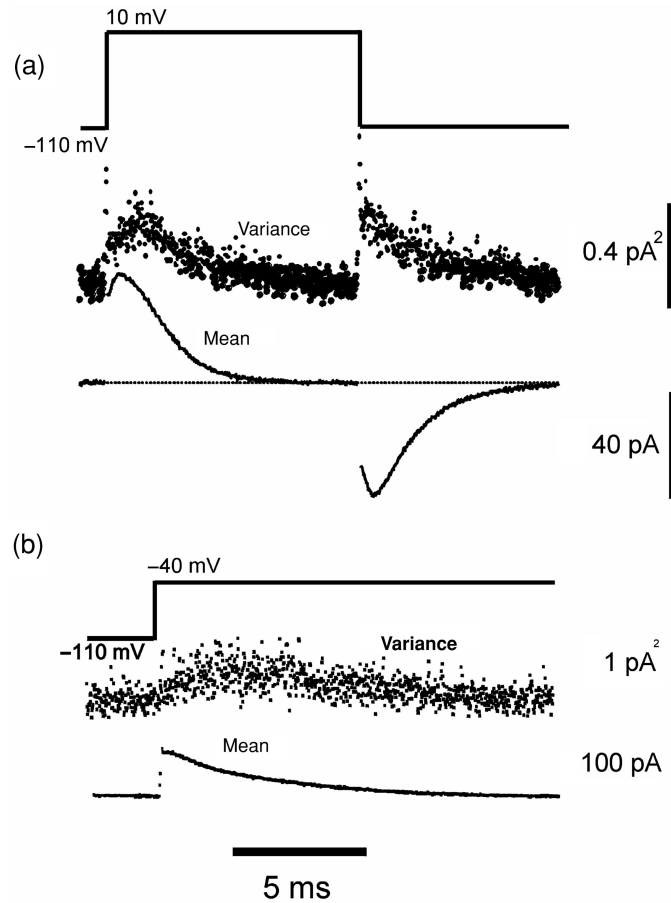


Fig. 3.7 Current fluctuations in gating currents. (a) Top trace is the time course of a pulse to +10 mV, middle trace is the variance and bottom trace is the mean computed from several hundred traces. (b) Top trace is the time course of a smaller pulse to -40 mV, middle trace is the variance and lower trace is the mean computed from hundreds of traces. Modified from Sigg et al. (1994).

indicates that at early times the elementary event is smaller than at longer times. The gating current decreases with two exponential components, which are more separated in time at small depolarizations. Therefore, it is possible to attribute the small shots to the fast component and the large shots to the slow component. This would indicate that the early transitions of the gating current are made up of several steps each carrying a small elementary charge. The total movement of charge in the early transitions would have to account for the $3.6 e_0$ needed to make the total of $13 e_0$ per channel. We conclude from these experiments that the gating current of a single channel is made up of small shots at early times followed big shots of currents that in the average gating current show two exponential decays.

3. Voltage-Gated Ion Channels

3.5 Structural Basis of the Gating Charges

In this section, we will address the relation between the function of the voltage sensor and its structural basis. We will first ask where are the charges or dipoles in the structure of the channel and then how those charges or dipoles move in response to changes in membrane potential.

3.5.1 The Structures Responsible for the Gating Charge Movement

There are many ways one could envision how the charge movement is produced by the channel protein. The putative α -helical transmembrane segments have an intrinsic dipole moment that upon tilting in the field would produce an equivalent charge movement. Also, induced dipoles of amino acids side chains could accomplish the same. However, $13 e_0$ per channel is very large and charged amino acids become the most likely possibility. Since the first channel was cloned, it was recognized that the S4 segment with its basic residues would be the prime candidate for the voltage sensor (Noda et al., 1984). By introducing mutations that neutralize the charges in S4, several studies found that there were clear changes in the voltage dependence of the conductance. However, shifts in the voltage dependence of the P_o-V curve or even apparent changes in slope in the voltage range of detectable conductance do not prove that charge neutralization is decreasing the gating charge. The proof requires the measurement of the charge per channel (z_T) for each one of the neutralizations. If after neutralization of a charged residue the charge per channel decreases, one may assume such charge is part of the gating current. Using the methods to measure total charge per channel discussed above in Shaker, two groups found that the four most extracellular positive charges in S4 (Aggarwal and MacKinnon, 1996; Seoh et al., 1996) and that one negative charge in the S2 segment were part of the gating charge (Seoh et al., 1996) (see white symbols in Fig. 3.1). It is interesting to note that in several instances a neutralization of one particular residue decreased the total gating charge by more than $4 e_0$. This indicates that somehow the charges interact with the electric field where they are located such that the elimination of one charge can affect the field seen by the remaining charges. If most of the gating charge is carried by the S4 segment ($4 e_0$ per subunit), it gives a total of $16 e_0$. Therefore, to account for the $13 e_0$ for the total channel obtained from charge/channel measurements, they all must move at least 81% of the membrane electric field ($16 \times 0.81 = 13$).



3.5.2 Movement of the Charges in the Field

Knowing the residues that make up the gating charge is a big advance because it makes it possible to test their positions as a function of the voltage and thus infer the possible conformational changes.

As we will see below, the literature contains a large number of papers (for reviews, see Yellen, 1998; Bezanilla, 2000) with many types of biophysical experiments

Francisco Bezanilla

testing the accessibility, movement and intramolecular distance changes. With all these data, several models of the voltage sensor movement were proposed that could account for all the experimental observations but in total absence of solid information on the three-dimensional structure of the channel. In the next section, we will discuss many of the biophysical measurements of the voltage sensor and the models that have emerged from them and the recently solved crystal structures of KvAP (Jiang et al., 2003a) and Kv1.2 (Long et al., 2005a).

3.6 Structural Basis of the Voltage Sensor

A three-dimensional structure of the channel, even in only one conformation, would be invaluable as a guideline in locating the charges inside the protein and in proposing the other conformations that account for the charge movement consistent with all the biophysical measurements. We will see below that the first solved crystal structure of a voltage-dependent channel available is not in a native conformation but just recently, a second crystal structure from a mammalian voltage-gated K channel (Kv1.2) appears to be closer to its expected native conformation. In any case, in both cases the crystals are in only one conformation (open inactivated). Therefore, we are still relying on data that can only be used to propose models because the information on the three-dimensional structure of the channel is still uncertain and incomplete.

3.6.1 Crystal Structures of Voltage-Dependent Channels

The long awaited first crystal structure of a voltage-dependent channel, KvAP from *archaea Aeropyrum pernix*, was published by the MacKinnon group (Jiang et al., 2003a). The structure was a surprise because it showed the transmembrane segments in unexpected positions with respect to the inferred bilayer. For example, the N-terminal was buried in the bilayer whereas it has been known to be intracellular; the S1–S2 linker is also buried although it has been previously shown to be extracellular. The S4 segment, along with the second part of S3 (S3B) formed the paddle structure that was intracellular and lying parallel to the bilayer, a location that would be interpreted as the closed position of the voltage sensor. However, the pore gates in the same crystal structure clearly corresponded to an open state. Thus, the crystal structure is in a conformation that was never observed functionally, raising the question whether that crystal structure of KvAP is indeed representative of the native conformation of the channel in the bilayer. The authors functionally tested the structure by incorporating the channel in bilayers and recording the currents through the channel after Fab fragments were added to the inside or to the outside of the channel. The Fab fragment did not attach from the inside but only from the outside, showing that the position of the S3–S4 shown in the crystal structure (obtained in detergent) did not represent a native conformation of the channel in the bilayer (Jiang et al., 2003b).

3. Voltage-Gated Ion Channels

Along with the crystal structure of the full KvAP channel, Jiang et al. (2003a) solved the crystal structure of the S1 through S4 region of KvAP (the isolated voltage sensor). This crystal showed similarities but was not identical to the S1–S4 region of the full KvAP crystal structure (Cohen et al., 2003). This second crystal was docked to the pore region of the full crystal to obtain two new structures that were proposed in the open and closed conformations as the *paddle model* of channel activation. It is important to note here that the structures shown in the second paper (Jiang et al., 2003b) do not correspond to the original KvAP structure. In fact, the proposed structures of the model depart so much from the crystal structure that we should treat them just like any other model of activation proposed before.

A recent paper by Long et al. (2005a) reporting the crystal structure of the Kv1.2 channel in the open-slow-inactivated state shows an arrangement of the transmembrane segments that is dramatically different from KvAP but at the same time much closer to the inferred structure from previous biophysical results.

3.6.2 Models of Sensor Movement

A compact way of reviewing the large body of biophysical information on structural changes of the voltage sensor is to describe the models that are currently proposed to explain the operation of the voltage sensor.

Figure 3.8 shows schematically three classes of model that have been proposed to explain the charge movement in voltage-dependent channels. In all cases, only two of the four sensors are shown and the coupling from the sensor to the gate is not shown explicitly. In addition, the charge that moves resides completely in the first four charges of the S4 segment. The common feature of all three models is that the charge is translocated from the inside to the outside upon depolarization. However, there are important differences as of how those charges relocate in the protein structure.

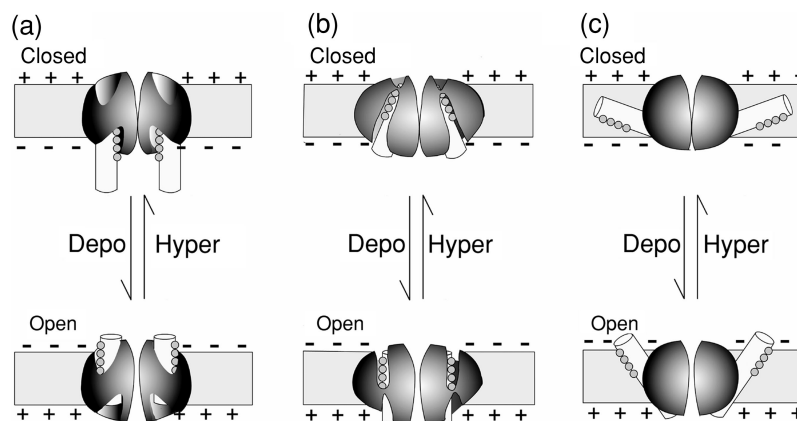


Fig. 3.8 Three models of the voltage sensor. (a) Helical screw model, (b) Transporter model, (c) Paddle model. The charged residues are shown as gray circles. For details see text.

Francisco Bezanilla

Figure 3.8a shows the conventional *helical screw* model (Caterall, 1986; Durell and Guy, 1992). Although there are variations on this model, the general idea is that upon depolarization the S4 segment rotates along its axis and at the same time translates as a unit perpendicular to the membrane, thus changing the exposure of the charges from the intracellular to the extracellular solution, effectively translocating $4 e_0$ per subunit (see Fig. 3.8a). In the original version of the model the change of exposure required a large 16 \AA translocation of the S4 segment and the positively charged arginines were making salt bridges with aspartate or glutamates residues that had to be broken to initiate the movement. In more recent versions (Gandhi and Isacoff, 2002; Ahern and Horn, 2004a,b; Durell et al., 2004) the charges are in water crevices in both the closed and open position, decreasing the amount of translation required of the S4 segment.

Figure 3.8b shows the *transporter* model (Bezanilla, 2002; Starace and Bezanilla, 2004; Chanda et al., 2005). In the closed position, the charges are in a water crevice connected to the intracellular solution and in the open position they are in another water crevice connected to the extracellular solution. The translocation of the charges is achieved by a tilt and rotation of the S4 segment with little or no translation. In this case the field is concentrated in a very small region that changes from around the first charge in the closed state to the fourth charge in the open state.

Fig. 3.8c shows the *paddle* model introduced by the MacKinnon group (Jiang et al., 2003b) where the S4 segment is located in the periphery of the channel and the charges are embedded in the bilayer. The S4 segment makes a large translation such that the most extracellular charge goes from exposed to the extracellular medium in the open state to completely buried in the bilayer in the closed state.

The helical screw and transporter models are similar but they differ dramatically from the paddle model in that the gating charges in the paddle model are embedded in the bilayer while in the helical screw and transporter models the charges are surrounded by water, anions or making salt bridges. In contrast with the transporter model, the helical screw model has in common with the paddle model the large translation of the S4 segment.

In the following sections, we will review biophysical experiments that were designed to test the topology of the channel and the extent of the conformational changes of the gating charge. In the absence of a native crystal structure in the open and closed conformations, these experiments are the data that we can use to support or reject the available models of voltage sensor operation.

3.6.3 The Topology of the Channel and Gating Charge Location

Alanine and tryptophan scanning have been used to infer the relative positions of the transmembrane segments (Monks et al., 1999; Li-Smerin et al., 2000) and the results indicate that the S1 segment is in the periphery of the channel. This result is at odds with the recent report by Cuello et al. (2004) where using electron paramagnetic resonance (EPR) scanning, they found that in KvAP the S1 segment is not exposed to the bilayer but rather surrounded by the rest of the protein. This

3. Voltage-Gated Ion Channels

difference could be an inherent limitation in the ala or trp scanning techniques that test the function of the channel or it could be a genuine difference between eukaryotic and prokaryotic channels. Recent results seem to confirm this last possibility. Using LRET measurements, Richardson et al. (2005, 2006) show that in both the prokaryotic voltage-gated channels NaChBac and KvAP the S1 segment is indeed close to the pore in agreement with the results of Cuello et al. (2004) and the recent structure of Long et al. (2005a) shows that in the eukaryotic Kv1.2 voltage-gated channel the S1 is closer to the periphery. With regard to the S4 segment, the results of Cuello et al. (2004) show that the S4 segment seems to be partially exposed to the bilayer, in agreement with the paddle model. However, in Cuello et al. (2004) the two innermost charged residues are protected by the protein and the two outermost charges are in the interface, contrary to the location proposed in the paddle model. The crystal structure of Kv1.2 confirms the results of Cuello et al. (2004) because the two inner charges are protected while the two outermost charges are in the interface. It is interesting to notice that the crystal of Kv1.2 show the two outermost arginines pointing into the bilayer but their alpha carbons are at 13 Å from the center of the bilayer, which corresponds to the polar part of the lipid bilayer. Recent molecular dynamics simulations of the Kv1.2 channel in a lipid bilayer shows that the first two arginines are completely hydrated (Roux, personal communication).

Laine et al. (2003) found that the extracellular part of the S4 segment gets within a few Ångströms of the pore region in the open state of Shaker-IR channel. This result is consistent with the helical screw and the transporter model but is inconsistent with the paddle model presented in (Jiang et al., 2003b) because in their model the extracellular portion of S4 is well separated from the rest of the channel protein giving a distance of about 98 Å between segments across the pore region. In experiments using resonance energy transfer with lanthanides (Cha et al., 1999a,b; Richardson et al., 2005) or with organic fluorophores (Glauner et al., 1999) that distance was found to be around 50 Å also in agreement with measurements done with tethered TEA derivatives (Blaustein et al., 2000). These results indicate that the S4 segment is not extended into the bilayer but it is against the bulk of the channel protein. If the paddle model were modified, so that the S4 segments would be almost perpendicular to the plane of the bilayer in the open state and almost parallel to the bilayer in the closed state but still flush against the rest of the protein it would be consistent with the distance constraints just mentioned. In another report, the MacKinnon group made such modification at least for the open-inactivated state (Jiang et al., 2004). The recent structure of Kv1.2 (Long et al., 2005a) shows that the S4 segment is indeed almost perpendicular to the plane of the membrane. However, even with these modifications the paddle model locates the charges in the bilayer, a proposal that is inconsistent with the EPR results (Cuello et al., 2004) and several other biophysical experiments (Fernandez et al., 1982; Yang and Horn, 1995; Larsson et al., 1996; Yang et al., 1996; Yusaf et al., 1996; Starace et al., 1997; Baker et al., 1998; Islas and Sigworth, 2001; Starace and Bezanilla, 2001; Asamoah et al., 2003, 2004; Starace and Bezanilla, 2004). Locating the charges in the bilayer has been a subject of intense debate because the energy required in moving a charge into

Au: The year 1999 has been changed into 1999a,b as per the reference list. Please delete whichever is not applicable.

Francisco Bezanilla

the low dielectric constant bilayer is extremely high (Parsegian, 1969). If positively charged gating charges are neutralized by making salt bridges with acidic residues, the energy decreases (Parsegian, 1969) but there would not be any gating charge movement. In a recent molecular dynamics simulation (Freites et al., 2005) the authors conclude that an isolated S4-like segment can be stabilized in a bilayer by making salt bridges between the arginines and the phosphates of the phospholipids producing a constricted 10 Å hydrophobic region. It is not clear from that structure what would be the charge translocated. Most importantly, the structure presented by Freites et al. (2005) is not a good model of the S4 in voltage-gated channels because it has been shown that the arginines are shielded (Cuello et al., 2004; Long et al., 2005a).

Evidence obtained by charge measurements in the squid axon sodium channel, have shown that the gating charges do not move in the bilayer (Fernandez et al., 1982). In these experiments addition of chloroform increased the kinetics of translocation of the hydrophobic ion dipicrylamine while it did not change the kinetics of the sodium gating currents. The conclusion was that the gating charge, unlike hydrophobic ions, does not move in the bilayer. Ahern and Horn (2004a,b) have explored this subject in more detail. As in the paddle model the S4 segment is in the bilayer, they reasoned that on addition of more charges in the S4 segment, the net gating charge should increase. Their results show that the charge addition at several positions did not increase the gating charge, indicating that only the charges in aqueous crevices are responsible for gating and can sense the changing electric field. Both these experimental results are hard to reconcile with the paddle model where the voltage sensor is immersed in the hydrophobic core of the lipid bilayer.

The S1–S2 loop has been clearly located in the extracellular region by several criteria. One is that a glycosylation site in Shaker occurs in this loop (Santacruz-Toloza et al., 1994). In addition, fluorescence signals from fluorophores attached in this loop are consistent with this region being extracellular (Asamoah et al., 2004), as well as the recent EPR scanning of KvAP (Cuello et al., 2004). These results are in agreement with the helical screw and transporter models but are again inconsistent with the location proposed in the paddle model. In the KvAP crystal structure the S1–S2 linker is buried in the bilayer with an S2 segment almost parallel and also buried in the bilayer. The recent crystal structure of Kv1.2, although not well resolved in this region, confirms that the S1–S2 loop is extracellular.

3.6.4 Voltage-Induced Exposure Changes of the S4 Segment and Its Gating Charges

Testing the exposure of the gating charges in the intra- or extracellular medium would give us an idea whether their voltage-induced movement takes them out of the protein core or from the lipid bilayer. There have been three different approaches to test exposure. The first method, cysteine scanning mutagenesis, consists of replacing the residue in question by a cysteine and then test whether a cysteine reagent can

3. Voltage-Gated Ion Channels

react from the extra- or intracellular solution and whether that reaction is affected by voltage (Yang and Horn, 1995; Larsson et al., 1996; Yang et al., 1996; Yusaf et al., 1996; Baker et al., 1998). The second method, histidine scanning mutagenesis, consists of titrating with protons the charge in the residues. In this case, as the pKa of the arginine is very high, histidine was used as a replacement allowing the titration in a pH range tolerated by the cell expressing the channel (Starace et al., 1997; Starace and Bezanilla, 2001, 2004). The third method consists of replacing the residue in question with a cysteine, followed by tagging it with a biotin group and then testing whether avidin can react from the inside or outside depending on the membrane potential (Jiang et al., 2003,a,b). The outcome of all these experiments is that indeed the charged residues in S4 undergo changes in exposure when the membrane potential is changed. However, it is important to look at each of these procedures with their limitations and compare their results because that may reveal many details of the actual movement of the charge.

3.6.4.1 Cysteine Scanning Mutagenesis

The experiments by Yang and Horn (1995) were the first to test the accessibility of charged groups to the extra- and intracellular solutions and its dependence on membrane potential. The idea of these experiments is to test whether a cysteine reacting moiety can attach to an engineered cysteine in the channel depending where the moiety is and what the electric field is. This method works provided the attachment induces a detectable change in the channel currents. In addition, the attachment of the moiety will depend on the local pH and state of ionization of the cysteine residue. Yang and Horn (1995) showed that the reaction rate of MTSET to the cysteine-replaced most extracellular charge of the S4 segment of the fourth domain of a sodium channel depended on membrane potential. To conclude that a particular site changes its exposure, the reaction rate must differ by more than an order of magnitude between the two conditions. This is important because if one just measures whether the reaction occurred or not, one may be sampling a rarely occurring conformational state. Their result showed for the first time that the accessibility of this group changed with voltage or alternatively that the ionization state was changed by voltage. This work was expanded to the deeper charges in the S4 segment of domain IV of the Na⁺ channel (Yang et al., 1996). The conclusion was that upon depolarization the most extracellular charge was exposed and that at hyperpolarized potential it became buried. In addition, the two following charges could be accessed from the inside at hyperpolarized potential and from outside at depolarized potential. The next two deeper charges were always accessible from the inside regardless of the membrane potential. These results strongly suggest that the three outermost charges change exposure with voltage and are consistent with the idea of a conformational change that translocates charges from inside to outside upon depolarization giving a physical basis to the gating currents.

These studies were also done in the Shaker-IR K⁺ channel (Larsson et al., 1996; Yusaf et al., 1996; Baker et al., 1998) and showed the same trend: the outermost

Au: The year 2003 has been changed into 2003a,b as per the reference list. Please delete whichever is not applicable.

Francisco Bezanilla

charges were exposed to the outside upon depolarization and the innermost to the inside on hyperpolarization. While some residues were inaccessible from one side to the cysteine-reacting compound on changing the voltage, there were a few that reacted when the reactive agent was added to the other side.

The conclusion from the cysteine scanning experiments is that the residues bearing the gating charges change their exposure with the voltage-dependent state of the channel. Another very important conclusion is that the charges are exposed to the solutions and not to the lipid bilayer since the SH group in the cysteine has to be ionized to react with the cysteine modifying reagent. This would be energetically unfavorable in the low dielectric medium of the bilayer. It is important to note that the reactivity of thiol groups on some of the sites tested was comparable to their reactivity in free solution.

3.6.4.2 Histidine Scanning Mutagenesis

Testing the titration of the charged residues is a direct way to address exposure of the charges to the solutions. In this approach, each arginine or lysine is exchanged to a histidine residue that can be titrated in a pH range that is tolerated by the expression system. The titration of the histidine with a proton can be easily detected as a change in the gating current, provided the ionic current is blocked. For this reason, most of these experiments were carried out in the nonconducting Shaker-IR K⁺ channel that bears the W434F mutation.

The logic of this procedure can be understood by taking some limiting cases. (i) If the histidine is not exposed to the solutions and/or if it does not move in the field, it would not be possible to titrate it from either side or under any membrane potential; therefore, no change in the gating currents are observed. (ii) The histidine can be exposed to the inside or to the outside depending on the membrane potential and thus on the conformation of the voltage sensor. In this case, if a pH gradient is established, every translocation of the voltage sensor would also translocate a proton, thus producing a proton current. This proton current would be maximum at potentials where the sensor is making most excursions, which occurs around the midpoint of the $Q-V$ curve. At extreme potentials, the gating current would be affected but no steady proton current would be observed. Therefore, the $I-V$ curve of such proton current would be bell-shaped. (iii) One particular conformation of the sensor locates the histidine as a bridge between the internal and external solutions forming a proton selective channel. In this case a steady current would be observed that would have an almost linear $I-V$ curve in the range of potentials where that conformation is visited and would be zero otherwise. The analysis of histidine scanning was done in Shaker-IR K⁺ channels and six charges were tested starting from the most extracellularly located (Starace et al., 1997; Starace and Bezanilla, 2001, 2004). Fig. 3.9a shows the results where the accessibility of each of the mutant is shown. The first four charges are accessible from both sides depending on the membrane potential, while the next two are not titratable.

3. Voltage-Gated Ion Channels

(a)

Mutant	Accessibility	Proton Current
R362H	both sides	pore
R365H	both sides	transporter
R368H	both sides	transporter
R371H	both sides	transporter/pore
K374H	not titratable	none
R377H	not titratable	none

(b)

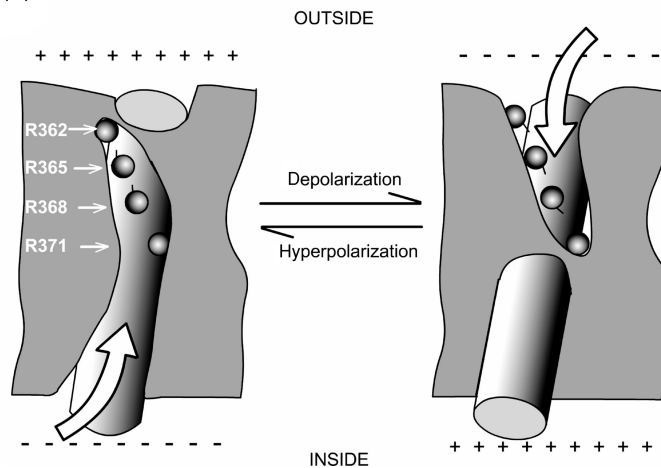


Fig. 3.9 Results of histidine scanning mutagenesis. (a) Each mutant is listed with the type of current observed and their accessibility to the internal and external solutions. In the case of K374H and R377H, the histidine may not be accessible and/or they do not move in the field. (b) Interpretation of the histidine scanning experiments with the transporter model based on a molecular model built with KvAP and KcsA crystal structures. A change in tilt of the S4 segment exposes the first four charges to the outside in the depolarized condition and to the inside in the hyperpolarized condition. In the hyperpolarized condition, there is a very narrow region bridged by histidine in position 362 and in the depolarized condition a bridge is formed by histidine in position 371. For details see text.

These results are consistent with what we know about the role of each charge. Only the first four charges, which are responsible for most of the gating charge, seem to translocate, while the next two either do not move in the field or are never accessible from the solution. The results also show that some of the charges that appeared buried to the cysteine scanning mutagenesis method are accessible to protons indicating that they are pointing into deep crevices that are too narrow for the cysteine-modifying reagent but large enough for protons to reach.

Figure 3.9b shows how the results could be explained in terms of an actual structure of the S4 segment with its associated membrane segments and bilayer, based on a transporter-like molecular model (Chanda et al., 2005) built with the

Francisco Bezanilla

crystal structures of KvAP and KcSA. The alpha-helical S4 segment is represented by a cylinder showing the first four charged arginines, as labeled. The next two arginines are on the back side of the S4 helix and are not visible. The hydrophobic region, that includes other segments and the bilayer, is simply shown as a gray area. In the closed state the first four charges are in contact with the internal solution by way of a water crevice (up arrow); however, the most extracellular charge (R362) is in the boundary between the intracellularly connected water crevice and the extracellular solution. If this arginine were replaced by a histidine it would form a proton pore by making a bridge between both solutions. Upon depolarization the S4 segment changes its tilt and all four charges become exposed to a water crevice (down arrow) connected to the extracellular solution. Now the fourth charge is in the boundary between the extra- and intracellular solutions so that a histidine in this position would form a proton pore. Notice that R365 (and also R368) change exposure in such a way that if each one were replaced by a histidine in the presence of a proton gradient, every transition would be able to shuttle one proton from one side to the other. It was found that R371H is a transporter but it can also form a proton pore at large depolarized potentials (Starace and Bezanilla, 2001).

The consequence of these results is that in the two extreme positions the electric field is concentrated (Islas and Sigworth, 2001) in a very narrow region of the protein: near 362 in the closed position and near 371 in the open position. This means that there is no need for a large movement of the voltage sensor to transport a large amount of charge. Asamoah et al. (2003) have shown that indeed the field is concentrated in this region by using a cysteine reactive electrochromic fluorophore. By attaching this fluorophore in different regions of the channel and comparing the fluorescence signal induced by voltage changes with the same electrochromic group in the bilayer, the field in the S4 region was found to be at least three times more intense. By attaching different lengths adducts to cysteine replacing position 362, Ahern and Horn (2005) have also estimated that the field at that position is concentrated. When residue 362 was replaced by alanine (Tombola et al., 2005) it was found that a current may be recorded at negative potentials (the ω current) a result that is consistent with the results of the 362H histidine pore and confirming the proposal that this region becomes extremely narrow at negative potentials.

The results of histidine and cysteine scanning experiments suggest that the charged arginine residues are stabilized by water and possible anions residing in the water filled crevices. It has been shown by Papazian and collaborators (Papazian et al., 1995; Tiwari-Woodruff, 1997) that the acidic residues in S2 and S3 segments play a stabilizing role in the structure of Shaker-IR channel but they could also lower the energy of the arginines in the crevices and possibly contribute to the gating charge by focusing the field in that region.

3.6.4.3 Biotin and Streptavidin Scanning

Biotin and its cysteine modifying derivative can react with cysteines engineered in the channel protein. In addition, the biotin group binds avidin, a large soluble



Au: The year 2004 has been changed into 2005 as per the reference list. Is this OK?

3. Voltage-Gated Ion Channels

protein molecule that is not expected to cross the membrane. Jiang et al. (2003b) studied several positions by mutating residues to cysteine in S3b and S4 segments of KvAP and attached to it a biotin molecule. After incorporating these channels into bilayers, they tested whether the currents were affected by avidin in the external or internal solutions. They found that, depending on the site of biotin attachment, the currents were decreased by externally or internally applied avidin. There were two sites (residues 121 and 122), lying in between the second and third charges of KvAP, where they saw inhibition by avidin from both sides. They indicated that in the conventional model (helical screw or transporter models) it would be extremely difficult to relocate the linker of the biotin along with the charges moving within the protein core. Therefore, they proposed that those sites must move a large distance within the bilayer to reach for the avidin present in the solution and gave them the basic restrictions on the extent that the paddle must move. Although this result is consistent with the paddle model, it is not inconsistent with the transporter model because those residues may in fact be facing the bilayer (Chanda et al., 2005) and thus allowing the biotin to reach to either side of the bilayer to attach to the avidin. It should be noted that no reaction rate was measured in those experiments (Jiang et al., 2003b) nor in the most recent paper (Ruta et al., 2005). Therefore, the accessibilities measured with avidin may well be the result of conformations that were rarely visited because the biotin–avidin reaction is essentially irreversible.

3.6.5 Fluorescence Spectroscopy Reveals Conformational Changes of the Voltage Sensor

Site-directed fluorescence is a powerful technique to follow conformational changes in a protein. In the case of voltage-dependent channels, the idea is to label specific sites of the channel protein with a fluorophore and measure changes in fluorescence induced by changes in the field. The salient feature of this technique is that the changes measured reflect local changes in or near the site where the fluorophore is located in the protein as opposed to electrical measurements that reflect overall conformations of the protein. Two main types of measurements have been done with site-directed fluorescence. One is the detection of fluorescence intensity changes of one fluorophore in the labeled site and the other is the estimation of distance and distance changes between two fluorophores using fluorescence resonance energy transfer (FRET).

3.6.5.1 Site-Directed Fluorescence Changes

In these experiments, the site of interest is mutated to a cysteine and then is reacted to a fluorophore that has a cysteine reactive group and the time course of fluorescence is monitored during pulses applied to open or close the channel (Mannuzzo et al., 1996; Cha and Bezanilla, 1997). To detect a fluorescence change, the conformational change must change the environment around the fluorophore so that the intensity changes because of spectral shifts, quenching or dye reorientation. In most cases the

Francisco Bezanilla

changes in fluorescence have been traced to changes in the quenching environment around the fluorophore (Cha and Bezanilla, 1997, 1998) and in a few cases it is produced by spectral shifts of the fluorophore as the hydrophobicity of the environment changes with the change in conformation (Asamoah et al., 2004). In some cases, the presence of quenching groups in the protein is crucial in obtaining a signal. For example, in the bacterial channel NaChBac the signals are very small or in some sites not detectable (Blunck et al., 2004) although, following the classical pattern, there are four charges in the S4 segment and the total gating charge was recently measured to be about $14 e_0$ (Kuzmenkin et al., 2004). This result has been traced to the lack of quenching groups in the structure of this channel (Blunck et al., 2004). To obtain signals from sites near the S4 segment upon changes of membrane potential, a requirement seems to be the presence of glutamate residues in the nearby region that act as quenching groups (Blunck et al., 2004).

Fluorescence changes in site-directed fluorescent labeling have provided information of local conformational changes around the S4 segment, the S3–S4 linker, S1–S2 linker and the pore region as a result of changes in membrane potential (Mannuzzu et al., 1996; Cha and Bezanilla, 1997; Loots and Isacoff, 1998). In the absence of three-dimensional structure, the interpretation of these fluorescence changes is not straightforward because the exact location of the fluorophore is unknown. However, several important qualitative results have been obtained. For example, it has been found that the kinetics of the fluorescence changes in S4 are slower than around the S1–S2 linker, suggesting that there might be earlier conformational changes that precede the main conformational change normally attributed to the S4 segment (Cha and Bezanilla, 1997). Also, the time course of fluorescence changes near the pore region are much slower than channel activation and their kinetics can be traced to another gating process called slow inactivation in Shaker K^+ channel (Cha and Bezanilla, 1997; Loots and Isacoff, 1998).

Probably one of the most informative results have been obtained in the sodium channel because, as this technique detects local changes, it has been possible to distinguish specific functions for each one of the four domains of the Na^+ channel. Fast inactivation is another gate that operates by blocking the channel pore (Hodgkin and Huxley, 1952; Armstrong and Bezanilla, 1977; Hoshi et al., 1990). By labeling the S4 segment of each domain of the Na^+ channel, it was found that the gating charge immobilization produced by inactivation only occurred in domains III and IV, thus locating the regions of the channel that interact with the inactivating particle (Cha et al., 1999a). The kinetics of the fluorescence of sites in S4 was found to be very fast in domains I–III but slower in domain IV, indicating that domain IV followed the other three domains (Chanda and Bezanilla, 2002). Finally, by comparing the effect of a perturbation in one domain to the fluorescence signal in another domain, it was found that all four domains of the Na^+ channel move in cooperative fashion. This result is important in explaining why sodium channels are faster than potassium channels, an absolute requirement in eliciting an action potential (Chanda et al., 2004). For more details on the voltage-dependent sodium channel, see the chapter by Hank in this volume.

3. Voltage-Gated Ion Channels

3.6.5.2 Resonance Energy Transfer

By labeling the protein with a donor and an acceptor fluorophore it is possible to estimate the distance between them using Förster theory of dipole–dipole interaction (Cantor and Schimmel, 1980). Depending on the fluorophore pair used, those distances can be from a few to about 100 Å, thus enabling the measurements of intramolecular distances and changes in distances.

This technique was used to estimate distances and distance changes between subunits in Shaker-IR channel by Cha et al. (1999b) and Glauner et al. (1999). Cha et al. (1999b) used a variant of FRET, called LRET that uses a lanthanide (terbium) as a donor and has the advantage that the estimation of the distances is more accurate mainly because the orientation factor is bound between tight limits giving a maximum uncertainty of $\pm 10\%$, but frequently is even better because the acceptor is not immobilized (Selvin, 2002). The LRET technique was tested and validated by Cha et al. (1999b) in the Shaker K⁺ channel where the measurement of distances between residues in the pore region gave an agreement within 1 Å when compared to an equivalent residue in the KcsA crystal structure. In addition, each measurement using LRET gave two distances that corresponded to the separation between adjacent and opposite subunits in the channel and those measured distances were related by the $\sqrt{2}$, as expected from the tetrameric structure, giving an internal calibration and consistency check of the technique.

Both studies (Cha et al., 1999b; Glauner et al., 1999) showed that the distances between S4 segments were around 50 Å and that it did not change very much from the closed to the open states. The maximum distance change measured by Cha et al. (1999b) was about 3 Å while Glauner et al. (1999) measured about 5 Å. These measurements were all done between subunits therefore they do not completely rule out a translation across the bilayer, as proposed in the helical screw and paddle models.

In Shaker K⁺ channel the linker between S3 and S4 is made of about 30 residues. At least six of the residues close to the extracellular part of S4 seem to be in alpha-helical conformation (Gonzalez et al., 2001) suggesting that S4 is extended extracellularly as an alpha helix. This would explain why Cha et al. (1999b) measured changes in distance in the S3–S4 linker as a result of membrane potential changes. One of those changes is a rotation in the linker and the other is a decrease in the tilt of the S4 with its extension upon depolarization, providing a possible mechanism for charge translocation (see Fig. 3.9).

The question of how much translation the S4 undergoes across the bilayer with depolarization has been approached with two other variants of FRET. In the first series of experiments (Starace et al., 2002) green fluorescent protein (eGFP) was inserted after the S6 of Shaker K⁺ channel and was used as the donor to an acceptor attached in the extracellular regions of the channel. In this case, the acceptor was a sulforhodamine with an MTS reactive group that can react with an engineered cysteine in the channel but it also can be cleaved off with a reducing agent. This allows the measurement of donor fluorescence (intracellularly located) in presence

Francisco Bezanilla

and absence of acceptor (in the extracellular regions of the channel) to compute the energy transfer and the distance. These measurements were done in multiple sites of the S1–S2 loop, S3–S4 loop, and S4 segment under depolarized and hyperpolarized conditions giving changes in distance that did not exceed 2 Å. In fact, some sites increased while others decreased their distance to the intracellular donor upon depolarization, indicating that there is little translation of the S4 across the membrane.

The second method used the hydrophobic negative ion dipyrilamine (dpa) as an acceptor that distributes in the edges of the bilayer according to the membrane potential (Fernandez et al., 1982; Chanda et al., 2005). The donor was rhodamine attached to specific sites in the S4 segment. The experiment predicts a clear distinction for the outcome depending whether the S4 does or does not make a large translation across the membrane. If the S4 segment undergoes a large translation across the bilayer such that the donor crosses its midpoint, then a *transient* fluorescence decrease is expected because dipyrilamine and the fluorophore start and end in opposite sides of the membrane but there is a period where both donor and acceptor reside simultaneously in both sides of the membrane increasing transfer and consequently decreasing donor fluorescence. On the other hand, if there is no crossing of the bilayer midline by the donor, the fluorescence will increase if the donor is above the midline or decrease if it is below, but no transient should be observed. The results of four sites in S4 are consistent with no crossing of the midline strongly suggesting that the S4 does not make a large translation upon depolarization (Chanda et al., 2005).

A recent detailed experiment using LRET confirms the lack of large translation of the S4 (Posson et al., 2005). In this case, the donor is Tb (in chelate form) attached in several sites of the S4 segment and the S3–S4 linker while the acceptor is in a toxin that blocks the pore of Shaker from the extracellular side. Results show that in all S4 sites measured the distance did not decrease more than 1 Å upon depolarization. When this change is projected as a translation of the S4 segment it gives an upper limit of only 2 Å.

It is interesting to note that in the LRET experiments using an acceptor in the toxin and a terbium chelate in the extracellular part of the S3 segment showed that in fact the distance *increased* by about 2 Å upon depolarization, which is also incompatible with the paddle model that postulates a simultaneous translation of S3 and S4 segments. Another confirmation that the extracellular part of S3 does not get buried in the closed state was provided by a recent paper by Gonzalez et al. (2004) who tested accessibility of these residues and found no state dependence.

Finally, another recent paper using a toxin that binds to the S3–S4 linker of the Shaker K channel also show that there is limited translation of the S4 segment (Phillips et al., 2005).

A recent molecular dynamic calculation of the voltage sensor of a K⁺ channel under the influence of an electric field also supports a conformational change that involves minimum translation (Treptow et al., 2004).

In summary, FRET experiments are inconsistent with a large transmembrane displacement of the S4 segment in response to a voltage pulse. As many other

Au: The year 2005 has been changed into 2001 as per the reference list. Is this OK?

3. Voltage-Gated Ion Channels

experiments, presented above and discussed in recent reviews (Bezanilla, 2002; Cohen et al., 2003; Ahern and Horn, 2004a,b; Swartz, 2004) do not support the idea that the charged residues are in the bilayer, the two main features of the paddle model become inconsistent with the available data.



3.7 Coupling of the Sensor to the Gate

In contrast to an FET where gating of the channel is produced by a change in space charge, the gate in voltage-gated channels seem to be a mechanical obstruction to flow (Yellen, 1998). The crystal structure of the bacterial channel KcSA reveals a closed state of the channel and Perozo et al. (1999) found that when it opens, the S6 makes a scissor-like action allowing ions to go through. The crystal structure of MthK, another prokaryotic channel, shows an open pore where a glycine in the S6 segment is shown to break the S6 in two segments (Jiang et al., 2002a). This led MacKinnon to propose that the gate opens when the S6 segment is broken and the intracellular part is pulled apart (Jiang et al., 2002b). In the crystal structure of the voltage-dependent prokaryotic channel KvAP the pore is in the open conformation by a break in the S6 segment in a glycine residue (Jiang et al., 2003a). In the case of the eukaryotic Shaker K⁺ channel there is a PVP sequence in the S6 segment that has been proposed to be the actual gate (Webster et al., 2004) and the crystal structure of Kv1.2 seems to indicate that the PVP motif is important. In addition to the main gate formed by the bundle crossing of the S6 segments, there is now very good evidence that the selectivity filter can also stop conduction, thus introducing another gate in series (Bezanilla and Perozo, 2003; Cordero et al., ~~submitted~~; Blunck et al., submitted). However, there is no evidence or a physical mechanism to couple this filter gate to the movement of the sensor.

The question of how and what kind of physical movement of the sensor, mainly the S4 segment, couples the opening of the pore gate is far from resolved. Most of the proposals, including the paddle model suggest that the change in position of the S4 couples via the intracellular S4–S5 linker to change the position of the S5 segment that in turns allow the opening of S6. The crystal structure of Kv1.2 suggests the same mechanism of opening whereby the S4 segment pulls on S5 to allow channel opening (Long et al., 2005b). In the transporter model (Chanda et al., 2005) the mechanism is more explicit because a closed and an open structures are proposed. In this case the change in tilt of the S4 segment carries the S5 segment away from S6 allowing the break at the glycine residue and thus opening the pore.

3.8 Concluding Remarks

The main component of the sensor of voltage-gated channels is the S4 segment with its basic residues moving in the field. The movement of the sensor in response to changes in the electric field produces the gating currents. The study of gating

Francisco Bezanilla

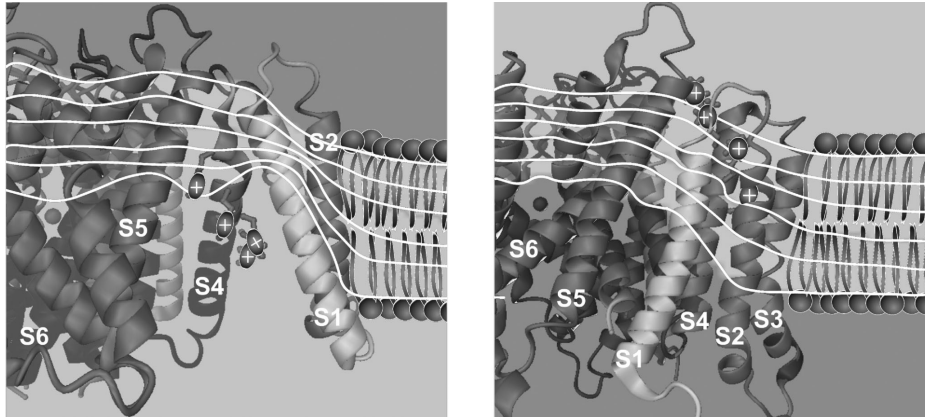


Fig. 3.10 The closed and open conformations and the voltage profile of the Shaker K^+ channel transporter model (Chanda et al., 2005). The isopotential lines divide equally the total voltage applied between the inside and the outside. (a) Closed state is obtained at hyperpolarized potentials (< -100 mV, clear inside). (b) Open state is obtained at depolarized potentials (> 50 mV, clear outside). Notice that going from a hyperpolarized to a depolarized potential, the S4 segment has not translated across the membrane but it has undergone a change in tilt that moves the position of S5 which in turn opens the pore by breaking S6. The arginines side chains relocate according to the direction of the field.

currents, single-channel currents, and macroscopic currents has generated detailed kinetic models of channel operation. The sensor couples to the gate possibly via the S4–S5 linker. The channel fully opens after all sensors have moved and there is little cooperativity in the early movements of the sensor in the K^+ channel but strong positive cooperativity in the Na^+ channel. The results of a large variety of biophysical experiments have helped in delineating the conformational changes of the sensor. These data have shown that the S4 segment does not undergo a translational motion across the membrane. Rather, the charges are in water crevices and they only move a small distance because the field is focused in a narrow region within the protein core. In the absence of a crystal structure representative of the channel in its native form in the closed state, we believe that the data support the transporter model.

The essence of the transporter model is the shaping of the electric field that allows the hydration of the arginines in the closed and active conformations of the sensor. As the field is concentrated in a small region of the protein, the movement of the charged arginines is much less than if they were to move in the hydrophobic part of the membrane. Fig. 3.10 shows a detail of the Shaker K channel model in the closed and active conformations as proposed by Chanda et al. (2005). In the closed state there is a large water crevice that penetrates the protein from the intracellular side, thus concentrating all the voltage drop in a narrow region close to the extracellular side (Fig. 3.10a). In this conformation, most of the arginines are in this water crevice but the most extracellular arginine is still within the field. Upon depolarization, the

3. Voltage-Gated Ion Channels

most extracellular arginine senses the change in field and tends to move out thus changing the tilt of the S4 segment as whole. This makes the intracellular crevice decrease locating the other arginines in the field, which will also help moving the S4 segment. Eventually, the internal crevice disappears and a small crevice appears in the extracellular side where the arginines will swing into it (Fig. 3.10b). The whole process involves a solid body motional tilt of the S4, most likely in several steps, and rearrangements of the arginine side chains giving a net transport of charge from the inside to the outside. There is almost no translation of the S4 across the plane of the membrane but there is a significant change in tilt that rearranges many other parts of the protein. In the resting state the extracellular portion of the S3 segment acts as a dielectric cover over the internal crevice and upon depolarization it moves away thus exposing the extracellular cavity that receives the guanidinium group of the arginines. Chanda et al. (2005) used the two proposed molecular structures (closed and open) to compute the net transfer of charge across the membrane solving the Poisson–Nernst–Planck equations (Roux, 1997). The result was a total of $13 e_0$, in excellent agreement with experimental data and the solution showed that the most of the charge was contributed by the first four most extracellular arginines of the channel (residues 362, 365, 368, and 371). The explicit molecular models of the closed and open states presented in Chanda et al. (2005) are based on a multitude of biophysical data and the available structural data. At present, these structures and the associated mechanism of the conformational change induced by membrane potential changes should be viewed as a representation of a conceptual model. Details of the positions of each of the relevant residues and their side chains and their trajectories during activation will be required to have a complete description of the voltage sensor operation.

3.9 Outlook

A detailed understanding of voltage-gated channels means that we can represent the landscape of energy of the physical states of the channel at atomic resolution together with the structural changes evoked by the electric field. To achieve this goal, it will not only require a static, high-resolution three-dimensional structure, but also a detailed description of the kinetics of the voltage-induced conformational changes. The latter are expected to be obtained with spectroscopic and computational techniques. Fluorescence and EPR spectroscopies have started to unravel some of the details of conformational changes during gating but the study of detailed kinetics is still developing. For example, in the same way that single-channel current recordings were critical in understanding the operation of the pore and the gate, single molecule fluorescence is expected to show the local conformational changes during voltage sensor operation and channel gating. These techniques are advancing very rapidly and some results have already been published as just the conformational change (Blunck and Bezanilla, 2002; Sonnleitner et al., 2002) or even correlated to current recordings (Blunck et al., 2003; Borisenko et al., 2003).

Francisco Bezanilla

Acknowledgments

Many thanks to Drs. Rikard Blunck and Baron Chanda for reading the manuscript and for their helpful and insightful comments. This work was supported in part by the U.S.P.H.S., N.I.H. under Grant GM30376.

References

- Aggarwal, S.K., and R. MacKinnon. 1996. Contribution of the S4 segment to gating charge in the *Shaker* K⁺ channel. *Neuron* 16:1169–1177.
- Agnew, W.S., S.R. Levinson, J.S. Brabson, and M.A. Raftery. 1978. Purification of the tetrodotoxin-binding component associated with the voltage-sensitive sodium channel from *Electrophorus electricus* electroplax membranes. *Proc. Natl. Acad. Sci. USA* 75:2602–2610.
- Ahern, C.A., and R. Horn. 2004a. Specificity of charge-carrying residues in the voltage sensor of potassium channels. *J. Gen. Physiol.* 123:205–216.
- Ahern, C.A., and R. Horn. 2004b. Stirring up controversy with a voltage sensor paddle. *Trends Neurosci.* 27(6):303–307.
- Ahern, C.A., and R. Horn. 2005. Focused electric field across the voltage sensor of potassium channels. *Neuron* 48:25–29.
- Almers, W. 1978. Gating currents and charge movements in excitable membranes. *Rev. Physiol. Biochem. Pharmacol.* 82:96–190.
- Armstrong, C.M., and F. Bezanilla. 1973. Currents related to movement of the gating particles of the sodium channels. *Nature* 242:459–461.
- Armstrong, C.M., and F. Bezanilla. 1977. Inactivation of the sodium channel. II. Gating current experiments. *J. Gen. Physiol.* 70:567–590.
- Asamoah, O.K., B. Chanda, and F. Bezanilla. 2004. A spectroscopic survey of gating-induced environmental changes in the Shaker potassium channel. *Biophys. J.* 86:432a.
- Asamoah, O.K., J.P. Wuskell, L.M. Loew, and F. Bezanilla. 2003. A fluorometric approach to local electric field measurements in a voltage-gated ion channel. *Neuron* 37:85–97.
- Baker, O.S., H.P. Larsson, L.M. Mannuzzu, and E.Y. Isacoff. 1998. Three transmembrane conformation and sequence-dependent displacement of the S4 domain in Shaker K⁺ channel gating. *Neuron* 20:1283–1294.
- Bezanilla, F. 2000. The voltage sensor in voltage-dependent channels. *Phys. Rev.* 80:555–592.
- Bezanilla, F. 2002. Perspective: Voltage sensor movements. *J. Gen. Physiol.* 120:465–473.
- Bezanilla, F., and E. Perozo. 2003. The voltage sensor and the gate in ion channels. *In: Advances in Protein Chemistry*, Vol. 63. D. Rees, editor. Elsevier Science, New York.

3. Voltage-Gated Ion Channels

- Bezanilla, F., E. Perozo, and E. Stefani. 1994. Gating of Shaker K⁺ channels. II. The components of gating currents and a model of channel activation. *Biophys. J.* 66:1011–1021.
- Blaustein, R.O., P.A. Cole, C. Williams, and C. Miller. 2000. Tethered blockers as molecular ‘tape measures’ for a voltage-gated K⁺ channel. *Nat. Struct. Biol.* 7:309–311.
- Blunck R., and F. Bezanilla. 2002. Fluorescence recordings of a low number of voltage gated K⁺ channels. *Biophys. J.* 82:267a.
- Blunck R., J. Cordero, L. Cuello, E. Perozo, and F. Bezanilla. 2006. Detection of the opening of the bundle crossing in KcsA with fluorescence lifetime spectroscopy reveals the existence of two gates for ion conduction (submitted).
- Blunck, R., D.M. Starace, A.M. Correa, and F. Bezanilla. 2004. Detecting rearrangements of *Shaker* and NaChBac in real-time with fluorescence spectroscopy in patch-clamped mammalian cells. *Biophys. J.* 86:3966–3980.
- Blunck, R., J.L. Vazquez-Ibar, Y.S. Liu, E. Perozo, and F. Bezanilla. 2003. Fluorescence measurements of KcsA channels in artificial bilayers. *Biophys. J.* 84(2, Pt 2):124a–125a.
- Borisenko, V., T. Loughheed, J. Hesse, E. Fureder-Kitzmuller, N. Fertig, J.C. Behrends, G.A. Woolley, G.J. Schutz. 2003. Simultaneous optical and electrical recording of single gramicidin channels. *Biophys. J.* 84(1):612–622.
- Cantor, C.R., and P.R. Schimmel. 1980. Biophysical Chemistry. Part II. Techniques for the Study of Biological Structure and Function. W.H. Freeman and Co., New York.
- Caterall, W.A. 1986. Molecular properties of voltage-sensitive sodium channels. *Annu. Rev. Biochem.* 55:953–985.
- Cha, A., and F. Bezanilla. 1997. Characterizing voltage-dependent conformational changes in the *Shaker* K⁺ channel with fluorescence. *Neuron* 19:1127–1140.
- Cha, A., and F. Bezanilla. 1998. Structural implications of fluorescence quenching in the *Shaker* K⁺ channel. *J. Gen. Physiol.* 112:391–408.
- Cha, A., P.C. Ruben, A.L. George, E. Fujimoto, and F. Bezanilla. 1999a. Voltage sensors in domains III and IV, but not I and II, are immobilized by Na⁺ channel fast inactivation. *Neuron* 22: 73–87.
- Cha, A., G. Snyder, P.R. Selvin, and F. Bezanilla. 1999b. Atomic scale movement of the voltage-sensing region in a potassium channel measured via spectroscopy. *Nature* 402:809–813.
- Chanda, B., O.K. Asamoah, and F. Bezanilla. 2004. Coupling interactions between voltage sensors of the sodium channel as revealed by site-specific measurements. *J. Gen. Physiol.* 123:217–230.
- Chanda, B., O.K. Asamoah, R. Blunck, B. Roux, and F. Bezanilla. 2005. Gating charge displacement in voltage-gated channels involves limited transmembrane movement. *Nature* 436:852–856.
- Chanda, B., and F. Bezanilla. 2002. Tracking voltage-dependent conformational changes in skeletal muscle sodium channel during activation. *J. Gen. Physiol.* 120:629–645.



Au: Please update this reference.

Francisco Bezanilla

- Chapman, M.L., and A.M.J. VanDongen. 2005. K channel subconductance levels result from heteromeric pore conformations. *J. Gen. Physiol.* 126:87–103.
- Cohen, B.E., M. Grabe, and L.Y. Jan. 2003. Answers and questions from KvAP structure. *Neuron* 39:395–400.
- Conti, F., and W. Stuhmer. 1989. Quantal charge redistribution accompanying the structural transitions of sodium channels. *Eur. Biophys. J.* 17:53–59.
- ~~Cordero, J., L.G. Cuello, Y. Zhao, V. Jogini, S. Chakrapani, B. Roux, and E. Perozo. 2005 (submitted).~~
- Cuello, L.G., M. Cortes, and E. Perozo. 2004. Molecular architecture of the KvAP voltage dependent K⁺ channel in a lipid bilayer. *Science* 306:491–495.
- Durell, S.R., and H.R. Guy. 1992. Atomic scale structure and functional models of voltage-gated potassium channels. *Biophys. J.* 62:238–250.
- Durell, S.R., I.H. Shrivastava, and H.R. Guy. 2004. Models of the structure and voltage-gating mechanism of the Shaker K⁺ channel. *Biophys. J.* 87:2116–2130.
- Fernandez, J.M., F. Bezanilla, and R.E. Taylor. 1982. Effect of chloroform on the movement of charges within the nerve membrane. *Nature* 297:150–152.
- Freites, J.A., D.J. Tobias, G. von Heijne, and S.H. White. 2005. Interface connections of a transmembrane voltage sensor. *PNAS* 102:15059–15064.
- Gandhi, C.S., and E.Y. Isacoff. 2002. Molecular models of voltage sensing. *J. Gen. Physiol.* 120:455–463.
- Glauner, K.S., L.M. Mannuzzu, C.S. Gandhi, and E.Y. Isacoff. 1999. Spectroscopic mapping of voltage sensor movements in the Shaker potassium channel. *Nature* 402:813–817.
- Gonzalez, C., E. Rosenman, F. Bezanilla, O. Alvarez, and R. Latorre. 2001. Periodic perturbations in Shaker K⁺ channel gating kinetics by deletions in the S3–S4 linker. *Proc. Natl. Acad. Sci.* 98:9617–9623.
- Hamill, O.P., A. Marty, E. Neher, B. Sackmann, and F.J. Sigworth. 1981. Improved patch-clamp techniques for high-resolution current recording from cells and cell-free membrane patches. *Pflugers Arch.* 391:85–100.
- Hirschberg, B., A. Rovner, M. Lieberman, and J. Patlak. 1996. Transfer of twelve charges is needed to open skeletal muscle Na⁺ channels. *J. Gen. Physiol.* 106:1053–1068.
- Hodgkin, A.L., and A.F. Huxley. 1952. A quantitative description of membrane current and its application to conduction and excitation in nerve. *J. Physiol.* 117:500–544.
- Horn, R., S. Ding, and H.J. Gruber. 2000. Immobilizing the moving parts of voltage-gated ion channels. *J. Gen. Physiol.* 116:461–476.
- Horrigan, F.T., J. Cui, and R.W. Aldrich. 1999. Allosteric voltage gating of potassium channels I: mSlo ionic currents in absence of Ca²⁺. *J. Gen. Physiol.* 114:277–304.
- Hoshi, T., W.N. Zagotta, and R.W. Aldrich. 1990. Biophysical and molecular mechanisms of Shaker potassium channel inactivation. *Science* 250:533–538.

Au: Please
update this
reference.



3. Voltage-Gated Ion Channels

- Islas, L.D., and F.J. Sigworth. 2001. Electrostatics and the gating pore of *Shaker* potassium channels. *J. Gen. Physiol.* 117:69–89.
- Jiang, Y., A. Lee, J. Chen, M. Cadene, B.T. Chait, and R. MacKinnon. 2002a. Crystal structure and mechanism of a calcium-gated potassium channel. *Nature* 417:515–522.
- Jiang, Y., A. Lee, J. Chen, M. Cadene, B.T. Chait, and R. MacKinnon. 2002b. The open pore conformation of potassium channels. *Nature* 417:523–526.
- Jiang, Y., A. Lee, J. Chen, V. Ruta, M. Cadene, B.T. Chait, and R. MacKinnon. 2003a. X-ray structure of a voltage-dependent K(+) channel. *Nature* 423:33–41.
- Jiang, Y., V. Ruta, J. Chen, A. Lee, and R. MacKinnon. 2003b. The principle of gating charge movement in a voltage-dependent K⁺ channel. *Nature* 423:42–48.
- Jiang, Q.-X., D.-N. Wang, and R. MacKinnon. 2004. Electron microscopic analysis of KvAP voltage dependent K⁺ channel in an open conformation. *Nature* 430:806–810.
- Keynes, R.D., and E. Rojas. 1974. Kinetics and steady-state properties of the charged system controlling sodium conductance in the squid giant axon. *J. Physiol (Lond.)* 239:393–434.
- Kuzmenkin, A., F. Bezanilla, and A.M. Correa. 2004. Gating of the bacterial sodium channel NaChBac: Voltage dependent charge movement and gating currents. *J. Gen. Physiol.* 124:349–356.
- Laine, M., M.C. Lin, J.P. Bannister, W.R. Silverman, A.F. Mock, B. Roux, and D.M. Papazian. 2003. Atomic proximity between S4 segment and pore domain in *Shaker* potassium channels. *Neuron* 39:467–481.
- Larsson, H.P., O.S. Baker, D.S. Dhillon, and E.Y. Isacoff. 1996. Transmembrane movement of the *Shaker* K⁺ channel S4. *Neuron* 16:387–397.
- Lee, H.C., J.M. Wang, and K.J. Swartz. 2003. Interaction between extracellular Hanatoxin and the resting conformation of the voltage sensor paddle in KV channels. *Neuron* 40(3):527–536.
- Li-Smerin, Y., D.H. Hackos, and K.J. Swartz. 2000. Alpha-helical structural elements within the voltage-sensing region domains of a K⁺ channel. *J. Gen. Physiol.* 115:33–50.
- Long, S.B., E.B. Campbell, and R. MacKinnon. 2005a. Crystal structure of a mammalian voltage-dependent *Shaker* family K⁺ channel. *Science* 309:897–903.
- Long, S.B., E.B. Campbell, and R. MacKinnon. 2005b. Structural basis of electromechanical coupling. *Science* 309:903–908.
- Loots, E., and E.Y. Isacoff. 1998. Protein rearrangements underlying slow inactivation of the *Shaker* K⁺ channel. *J. Gen. Physiol.* 112:377–389.
- Mannuzzu, L.M., and E.Y. Isacoff. 2000. Independence and cooperativity in rearrangements of a potassium channel voltage sensor revealed by single subunit fluorescence. *J. Gen. Physiol.* 115:257–268.
- Mannuzzu, L.M., M.M. Moronne, and E.Y. Isacoff. 1996. Direct physical measure of conformational rearrangement underlying potassium channel gating. *Science* 271:213–216.

Au: Please cite
this reference
in the text.

Francisco Bezanilla

- Monks, S.A., D.J. Needleman, and C. Miller. 1999. Helical structure and packing orientation of the S2 segment in the Shaker K⁺ channel. *J. Gen. Physiol.* 113:415–423.
- Noceti, F., P. Baldelli, X. Wei, N. Qin, L. Toro, L. Birnbaumer, and E. Stefani. 1996. Effective gating charges per channel in voltage-dependent K⁺ and Ca²⁺ channel. *J. Gen. Physiol.* 108:143–155.
- Noda, M., S. Shimizu, T. Tanabe, T. Takai, T. Kayano, T. Ikeda, H. Takahashi, H. Nakayama, Y. Kanaoka, and N. Minamino. 1984. Primary structure of *Electrophorus electricus* sodium channel deduced from cDNA sequence. *Nature* 312:121–127.
- Papazian, D.M., X.M. Shao, S.-A. Seoh, A.F. Mock, Y. Huang, and D.H. Weinstock. 1995. Electrostatic interactions of S4 voltage sensor in Shaker K⁺ channel. *Neuron* 14:1293–1301.
- Parsegian, A. 1969. Energy of an ion crossing a low dielectric membrane: Solutions to four relevant electrostatic problems. *Nature* 221:844–846.
- Perozo, E., M. Cortes, and L.G. Cuello. 1999. Structural rearrangements underlying K⁺-channel activation gating. *Science* 285:73–78.
- Perozo, E., R. MacKinnon, F. Bezanilla, and E. Stefani. 1993. Gating currents from a non-conducting mutant reveal open-closed conformations in Shaker K⁺ channels. *Neuron* 11:353–358.
- Phillips, L.R., M. Milescu, Y. Li-Smerin, J.A. Midell, J.I. Kim, and K.J. Swartz. 2005. Voltage sensor activation with a tarantula toxin as cargo. *Nature* 436:857–860.
- Posson, D.J., P. Ge, C. Miller, F. Bezanilla, and P.R. Selvin. 2005. Small vertical movement of a K⁺ channel voltage sensor measured with luminescence energy transfer. *Nature* 436:848–851.
- Richardson, J., P. Ge, P.R. Selvin, F. Bezanilla, and D.M. Papazian. 2006. Orientation of the voltage sensor relative to the pore differs in prokaryotic and eukaryotic voltage-dependent potassium channels [abstract]. *Biophys. J.*
- Richardson, J., D.M. Starace, F. Bezanilla, and A.M. Correa. 2005. Scanning NaCh-Bac topology using LRET [abstract]. *Biophys. J.*
- Roux, B. 1997. Influence of the membrane potential on the free energy of an intrinsic protein. *Biophys. J.* 73:2980–2989.
- Ruta, V., J. Chen, and R. MacKinnon. 2005. Calibrated measurement of gating-charge arginine displacement in the KvAP voltage-dependent K⁺ channel. *Cell* 123:463–475.
- Santacruz-Tolozza, L., Y. Huang, S.A. John, and D.M. Papazian. 1994. Glycosylation of Shaker potassium channel protein in insect cell culture and in *Xenopus* oocytes. *Biochemistry* 33:5607–5613.
- Schoppa, N.E., K. McCormack, M.A. Tanouye, and F.J. Sigworth. 1992. The size of gating charge in wild-type and mutant Shaker potassium channels. *Science* 255:1712–1715.
- Schoppa, N.E., and F.J. Sigworth. 1998. Activation of Shaker potassium channels. III. An activation gating model for wild-type and V2 mutant channel. *J. Gen. Physiol.* 111:313–342.

 Please provide the volume number and a page range for this reference.
 Au: Please provide the volume number and a page range for this reference.

3. Voltage-Gated Ion Channels

- Selvin, P.R. 2002. Principles and biophysical applications of luminescent lanthanide probes. *Annu. Rev. Biophys. Biomol. Struct.* 31:275–302.
- Seoh, S.-A., D. Sigg, D.M. Papazian, and F. Bezanilla. 1996. Voltage-sensing residues in the S2 and S4 segments of the Shaker K⁺ channel. *Neuron* 16:1159–1167.
- Sigg, D., and F. Bezanilla. 1997. Total charge movement per channel: The relation between gating displacement and the voltage sensitivity of activation. *J. Gen. Physiol.* 109:27–39.
- Sigg, D., F. Bezanilla, and E. Stefani. 2003. Fast gating in the Shaker K⁺ channel and the energy landscape of activation. *PNAS* 100:7611–7615.
- Sigg, D., H. Qian, and F. Bezanilla. 1999. Kramers' diffusion theory applied to gating kinetics of voltage dependent channels. *Biophys. J.* 76:782–803.
- Sigg, D., E. Stefani, and F. Bezanilla. 1994. Gating current noise produced by elementary transition in Shaker potassium channels. *Science* 264:578–582.
- Sonnleitner, A., L.M. Mannuzzu, S. Terakawa, and E.Y. Isacoff. 2002. Structural rearrangements in single ion channels detected optically in living cells. *Proc. Natl. Acad. Sci. USA* 99(20):12759–12764.
- Starace, D.M., and F. Bezanilla. 2001. Histidine scanning mutagenesis of basic residues of the S4 segment of the Shaker K⁺ channel. *J. Gen. Physiol.* 117:469–490.
- Starace, D.M., and F. Bezanilla. 2004. A proton pore in a potassium channel voltage sensor reveals a focused electric field. *Nature* 427:548–552.
- Starace, D.M., P.R. Selvin, and F. Bezanilla. 2002. Resonance energy transfer measurements on transmembrane motion of Shaker K⁺ channel voltage sensing region. *Biophys. J.* 82:174a.
- Starace, D.M., E. Stefani, and F. Bezanilla. 1997. Voltage-dependent proton transport by the voltage sensor of the Shaker K⁺ channel. *Neuron* 19:1319–1327.
- Swartz, K.J. 2004. Towards a structural view of gating in potassium channels. *Nat. Rev. Neurosci.* 5:905–916.
- Tempel, T.M., D.M. Papazian, T.L. Schwarz, Y.N. Jan, and L.Y. Jan. 1987. Sequence of a probable potassium channel component encoded at Shaker locus in *Drosophila*. *Science* 237:770–775.
- Tiwari-Woodruff, S.K., C.T. Schulteis, A.F. Mock, and D.M. Papazian. 1997. Electrostatic interactions between transmembrane segments mediate folding of Shaker K⁺ channel subunits. *Biophys. J.* 72:1489–1500.
- Tombola, F., M.M. Pathak, and E.Y. Isacoff. 2005. Voltage-sensing arginines in a potassium channel permeate and occlude cation-selective pores. *Neuron* 45:379–388.
- Treptow, W., B. Maignret, C. Chipot, and M. Tarek. 2004. Coupled motions between the pore and voltage-sensor domains: A model for Shaker B, a voltage-gated potassium channel. *Biophys. J.* 87:2365–2379.
- Vandenberg, C.A., and F. Bezanilla. 1991. A sodium channel model of gating based on single channel, macroscopic ionic and gating currents in the squid giant axon. *Biophys. J.* 60:1511–1533.

Francisco Bezanilla

- Webster, S.M., D. Del Camino, J.P. Dekker, and G. Yellen. 2004. Intracellular gate opening in Shaker K⁺ channels defined by high-affinity metal bridges. *Nature* 428:864–868.
- Yang, N., A.L. George, and R. Horn. 1996. Molecular basis of charge movement in voltage-gated sodium channels. *Neuron* 16:113–122.
- Yang, N., and R. Horn. 1995. Evidence for voltage-dependent S4 movement in sodium channels. *Neuron* 15:213–218.
- Yellen, G. 1998. The moving parts of voltage-gated ion channels. *Quart. Rev. Biophys.* 31:239–295.
- Yusaf, S.P., D. Wray, and A. Sivaprasadarao. 1996. Measurement of the movement of the S4 segment during activation of a voltage-gated potassium channel. *Pflugers Arc. Eur. J. Physiol.* 433:91–97.
- Zagotta, W.N., T. Hoshi, J. Dittman, and R. Aldrich. 1994. Shaker potassium channel gating III: Evaluation of kinetic models for activation. *J. Gen. Physiol.* 103:321–362.